ALGORITHMS FOR REGIONAL STRUCTURE – PROGRESS AND APPLICATION

Robert B. Herrmann,[1] Charles J. Ammon, [2] Kiehwa Lee,[3] Hyun-Jae Yoo[3]

Saint Louis University,[1] Pennsylvania State University,[2] Seoul National University[3]

Sponsored by Defense Threat Reduction Agency

Contract No. DTRA01-00-C-0214

ABSTRACT

Significant progress has been made in the development and documentation of standardized algorithms for analysis of regional Earth structure. *Computer Programs in Seismology – 3.15* was released in February 2002 to the research community. This distribution includes the new program suites **surf96**, **rftn96** and **joint96** for determining crustal structure from the inversion of surface-wave dispersion and/or teleseismic P-wave receiver functions. The programs have been applied to regional data sets in eastern Turkey and in the Republic of Korea.

Receiver functions were determined at all current broadband station locations in Korea except for the Incorporated Research Institutions for Seismology (IRIS) INCN and the KSAR stations. The time domain deconvolution tool of Ligorria and Ammon (1999) provides stable, causal and consistent receiver functions for inversion. Except for the stations on two islands, the receiver functions are very similar, attesting to the uniformity of the crust on the southern part of the Korean peninsula. The receiver functions require a uniform velocity model for the crust with a sharp, within resolution, crust-mantle transition. A test of the new programs **rftn96** and **joint96** was made using the data set at the Seoul National University station – the initial inversions highlight the non-uniqueness of receiver function inversion unless *a priori* crustal model information or other independent data, such as surface-wave dispersion, are introduced.

Computer Programs in Seismology – 3.16 will be released at the 24th Seismic Research Review, September 2002. This version includes the following: wavenumber integration synthetics for transversely isotropic media, newly adapted programs for regional focal mechanism determination using surface wave radiation patterns and broadband waveforms. The programs can be used for determination of local structure and seismic event source parameters. An outline of new codes to be developed with continuing support will also be presented.

OBJECTIVE

The objective of this effort is to develop regional scale crustal models that are precise enough to be used for waveform inversion of regional signals to characterize the source. Waveform inversion, even at low frequencies, requires an earth model specification much more detailed than required for location. Waveform inversion is important since this is the only means of calibrating local magnitude scales to teleseismic observations. To accomplish this task software development is tied to the analysis of real data sets.

RESEARCH ACCOMPLISHED

R. Herrmann visited Seoul National University (SNU) in 2000 (5 days), 2001 (2 weeks) and 2002 (2 weeks) for the purpose of establishing a cooperative relationship that permits access to both Korean Meteorological Administration (KMA) and Korean Institute of Geology and Mining (KIGAM) broadband data. The P.I. works with the SNU graduate students in the analysis of data. This year's trip led to the acquisition of a large data set for receiver function determination.

The geology of Korea consists largely of Pre-Cambrian rocks, such as granite gneisses and other metamorphics. Two separate blocks of Paleozoic strata are found in South and North Korea. Korea is stable land with no active volcanoes and rare earthquake shocks, although the islands of Ullungdo (station ULL) and Chejudo (stations SOG SGP) are of volcanic origin. The Pre-Cambrian basement of the peninsula is tectonically related to that of Manchuria and China. The generalized geology map of the peninsula is shown in Figure 1.

KMA has recently installed a modern digital seismic network in South Korea. This network consists of broadband STS-2, short period SS-1 and Episensor accelerometer sensors. The broadband station locations are given in Table 1 and their locations are plotted in Figure 2. Some stations were moved in 2001 to avoid overlap with KIGAM stations, to provide more even geographical coverage and to occupy quieter sites.

Teleseismic data were collected from earthquakes in three regions: India-Pakistan-Afghanistan, Indonesia-Philippines, and the Aleutians. Preprocessing consisted of windowing, removing the linear trend, rotation of horizontals and highpass filtering at 0.02 Hz. P-wave receiver functions were computed using the Ligorria and Ammon (1999) time domain deconvolution using the program saciterd. A total of 1127 receiver functions were obtained for the 25-station network. One aspect of the Ligorria and Ammon (1999) algorithm is the computation of a goodness of fit parameter that indicates the fit of the predicted radial component to the observed as a percentage. Receiver functions were computed for each event using Gaussian filter parameters of 0.5, 1.0 and 2.5, corresponding to low pass corners of 0.15, 0.30 and 0.75 Hz, respectively.

To compare the individual station receiver functions, a stack of the better receiver functions was made for each station. The selection criterion was that the goodness of fit be 80% and 95% for Gaussian filter parameters 1.0 and 2.5. This sieved data set is used for receiver function inversion for each station. The stack was made irrespective of the ray parameter since it varied little among the observations. Figure 3 presents the stacked receiver functions for each of the two filters. The station code is given to the left and the number of qualified waveforms used in the stack is indicated to the right of each stack. The waveforms window is [-5, 25] seconds with respect to the direct-P contribution.

The receiver functions of each station are very similar except ULL, SOG and SGP, which are on islands. To focus on the slight differences in the receiver function at each station, the stacked similar receiver functions are superimposed in Figure 4 for each filter parameter. The rainbow color scheme is alphabetical with BRD - red and ULJ - blue. Slight difference seen in the amplitude of the first peak may indicate local variations in upper crustal velocities. The slight shift in the second peak may indicate slight differences in local crustal thickness. Both causes are enhanced in the third peak halfway down the trace.

Although the seismicity levels in South Korea are low, some efforts have been made to define the crustal velocity structure using existing seismic network data. Kim *et al* (1998), Kim and Lee (2001) and Yoo and Lee (2001) used these models as a starting point for their receiver function studies at the broadband stations sites in Korea. Except for the ULL, SOG and SGP stations, the models are similar, as they should be because of the similarity of receiver functions seen in Figures 3 and 4. In a different study, Song and Lee (2001) used the program VELEST with 178 P-wave first arrivals from 29 local earthquakes recorded from 1991-1998 by the KMA analog-telemetry network. The latter study was hampered by the small number of observations but concluded that the average crustal P-wave velocity in the southern part of the peninsula is 6.3 km/s, the upper mantle P-wave velocity is near 7.9 km/s and that the crustal thickness is about 33 km.

To test the new inversion code and the capability of receiver functions to uniquely define the crustal velocity structure, the initial focus was on the recordings at SNU (Seoul National University). Receiver functions from 31 events were inverted under the assumption that nothing was known about the crust. The initial model consisted of a layered halfspace with a layer thickness of 2.5 km, P- and S-wave velocities of 8.0 and 4.7 km/s, respectively. The inversion applied a differential smoothness constraint and ten iterations were performed. The inversion constraints were that the halfspace velocity and the Poisson ratio in each layer were fixed. Next the same inversion was performed using the stacked receiver functions for the station and the same final model resulted. As expected because of the detail permitted in the model, the receiver function fits of the stacked data were perfect. Figure 5 presents the results of this inversion.

Next the receiver function data were combined with the Stevens (1999) Rayleigh-wave group velocity estimates for the peninsula and inverted jointly using the new program **joint96**. The resultant model and comparison of the model predictions to the observations are presented in Figures 6 and 7. The receiver-function and joint inversions share a similar sharp discontinuity that defines the Moho because the receiver functions require this feature. The receiver function model has higher crustal velocities (Figure 8) than the joint inversion model.

The program **timmod96 was** used to compare predicted P-wave first-arrival times for a surface focus event for the Song and Lee (2001), **rftn96** and **joint96** models (Figure 9). The joint inversion model is similar to the VELEST model except for the 0.5 sec delay, which is caused by the lower velocities in the upper crust. The upper crust velocities are controlled by the Stevens (1999) dispersion estimates and seem low for an essentially exposed arcane structure. The shallow part of the VELEST model is not well controlled either because of the lack of data at short distances from shallow foci events. These time delays are crucial since then will control the apparent depths of shallow events.

CONCLUSIONS AND RECOMMENDATIONS

A significant receiver function data set is now available. The inversion programs work, although more testing is required to document an effective methodology for inversion. Future work by SNU graduate students will use the regional earthquake arrival time for 2000-2002 in another application of VELEST for joint hypocenter and 1-D crustal velocity model determination since sufficient data should now exist from the broadband, short-period and accelerometer networks operated by KMA. Dispersion studies will focus on using teleseismic surface wave recordings to define Rayleigh- and Love-wave phase velocity dispersion as well as local Rg waves recorded at short distances. The recurrence rate of magnitude 4 - 5 events in Korea indicate that recording for waveform inversion for source parameters will be available in the next few years. Continued work on the Korean broadband data will permit a robust specification of crustal structure.

ACKNOWLEDGEMENTS

The authors wish to thank the Korean Meteorological Administration and the Korean Institute for Geology and Mining for the use of their broadband seismic data.

REFERENCES

Ammon, C. J., G. Randall and G. Zandt (1990). On the nonuniqueness of receiver function inversions, *J. Geophys. Res.,* 95, No. B10, 15303-15318.

Julia, J., C. J. Ammon, R. B. Herrmann and A. M. Correig (2000). Joint inversion of receiver function and surface wave dispersion observations, *Geophys. J. Int.,* 143, 1-19.

Kim, S. G., S. K. Lee, M. S. Jun and I. B. Kang (1998). Crustal structure of the Korean Peninsula from broadband teleseismic records using receiver function, *Econ. Environ. Geol.,* 31, No. 1, 21-29.

Kim. S. G., and S. K. Lee (2001). Moho receiver function methods studies beneath the broadband stations using receiver functions in South Korea, Korea *Society of Hazard Mitigation,* 6, No. 1. 139-155.

Ligorria, J. P., and C. J. Ammon (1999). Iterative deconvolution of teleseismic seismograms and receiver function estimation, *Bull. Seism. Soc. Am.,* 89, 1395-1400.

Song, S., and K. Lee (2001). Crustal structure of the Korean peninsula by travel time inversion of local earthquakes, *J. Korean Geophysical Society,* 4, No. 1, 21-33.

Stevens, J. L. (2001). Global Rayleigh wave dispersion article, *PAGEOPH,* in press.

Yoo, H., and K. Lee (2001). Crustal structure under the Taejon (TJN) station by receiver function methods, *J. Korean Geophysical Society,* 4, No. 1, 35-46.

Table 1. Broadband station locations in Republic of Korea.

Name	Latitude	Longitude	Elevation	Comment
TJN	36.3805	127.3615	161	KIGAM
SNU	37.4509	126.9566	161	KIGAM
GKP	35.8863	128.6083	46.51	KIGAM
BGD	34.1569	126.5575	5.7	KIGAM
KSA	38.5953	128.3512		KIGAM
HDB	35.7307	129.4012	Borehole	KIGAM
PUS	35.1010	129.0339	69.23	KMA Closed and moved to BUS in 2001
TAG	35.8750	128.6194	57.64	KMA Closed and moved to DAG in 2001
SOG	33.2390	126.5671	50.47	KMA Closed and moved to SGP in 2001
CHU	37.8904	127.7308	120.00	KMA Closed and moved to CHC in 2001
TEJ	36.3681	127.3712	68.28	KMA Closed and moved to CHJ in 2001
SEO	37.4879	126.9188	33.51	KMA
SES	36.7893	126.4531	99.1	KMA
KWJ	35.1599	126.9910	213.0	KMA
KAN	37.7425	128.8893	25.91	KMA Closed and moved to DGY in 2001
ULJ	36.7021	129.4084	77.1	KMA
ULL	37.4738	130.9008	218	KMA
BUS	35.2487	129.1125	91	
DAG	35.7685	128.8970	262	
CHC	37.7775	127.8145	245	
CHJ	36.8730	127.9748	227	
DGY	37.6904	128.6742	791	
SGP	33.2587	126.4994	222	
BRD	37.9677	124.6303	169	New 2002

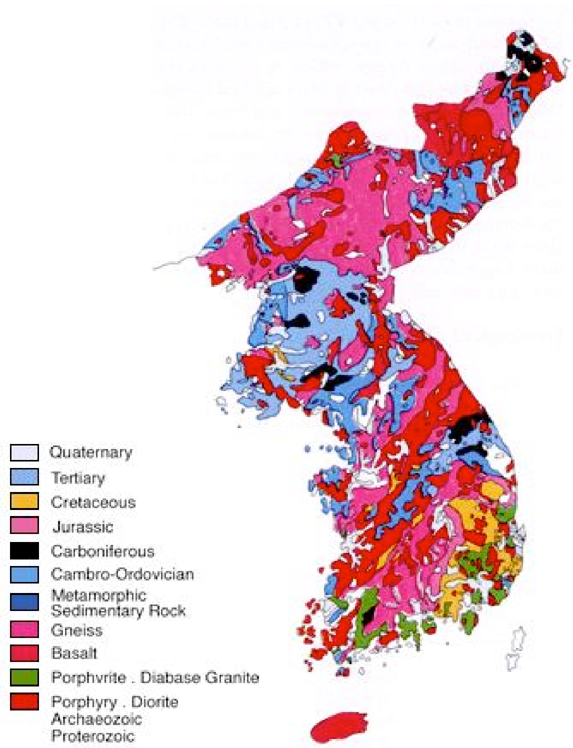

Figure 1. Geology of the Korean Peninsula http://cinema.sangji.ac.kr/WINDOW/window/win00000.htm

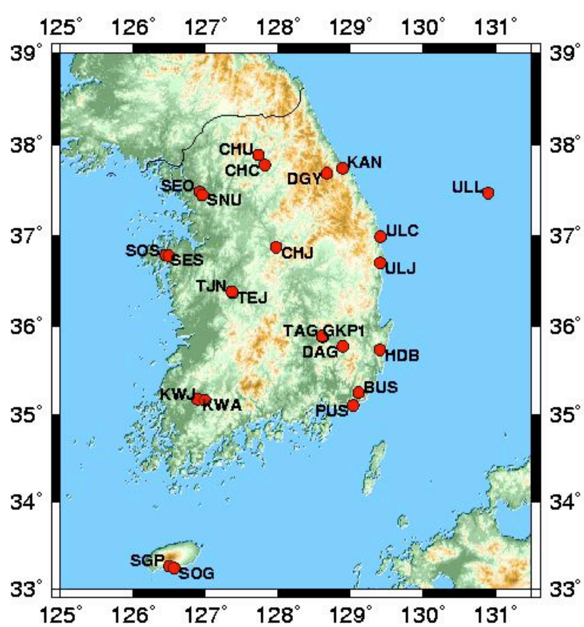

Figure 2. Location of broadband stations used in surface wave dispersion receiver function analysis of the Korean Peninsula.

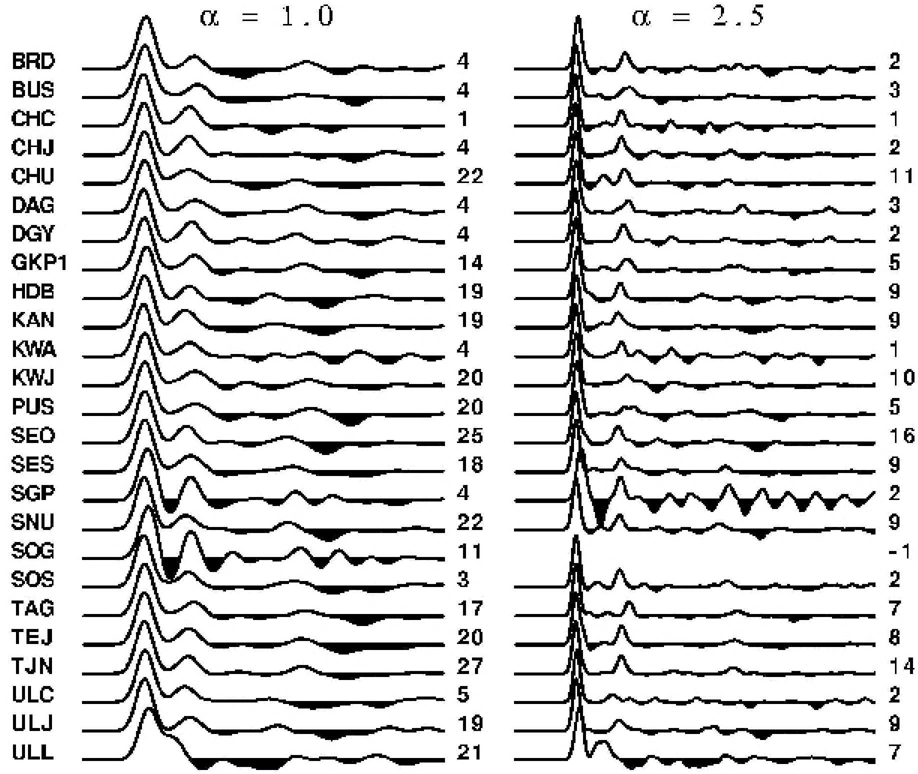

Figure 3. Stacked receiver functions all stations listed for each of the two Gaussian filter parameters. Traces begin 5 seconds before and 25 seconds after the direct P. The number to the right of each trace is the number of traces used in the stack.

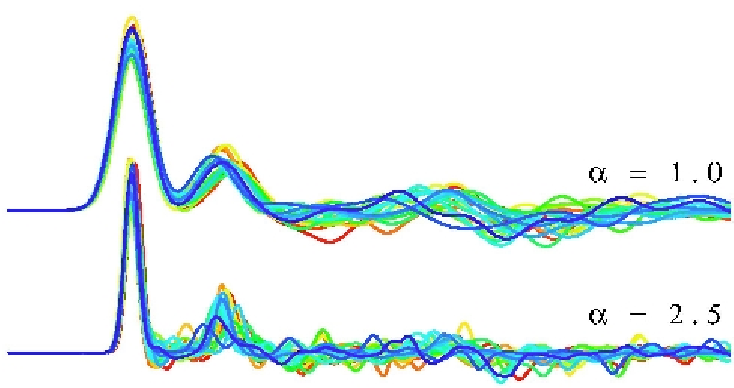

Figure 4. Overlay of stacked receiver functions for all stations except ULL, SOG and SGP. The color rainbow represents stations alphabetically with BRD 9red) and ULJ (blue). The time window is as above.

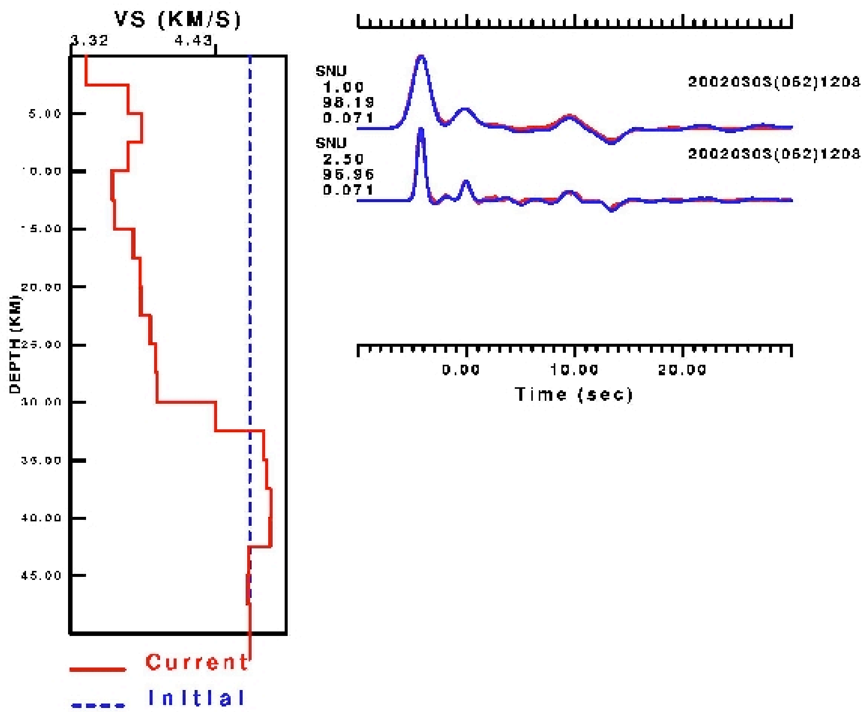

Figure 5. Inversion results using program rftn96 and the stacked receiver function data at SNU. The initial model is a uniform halfspace (blue). The final model is shown in red. The halfspace velocity was fixed. The model explains 97% of the observed receiver function.

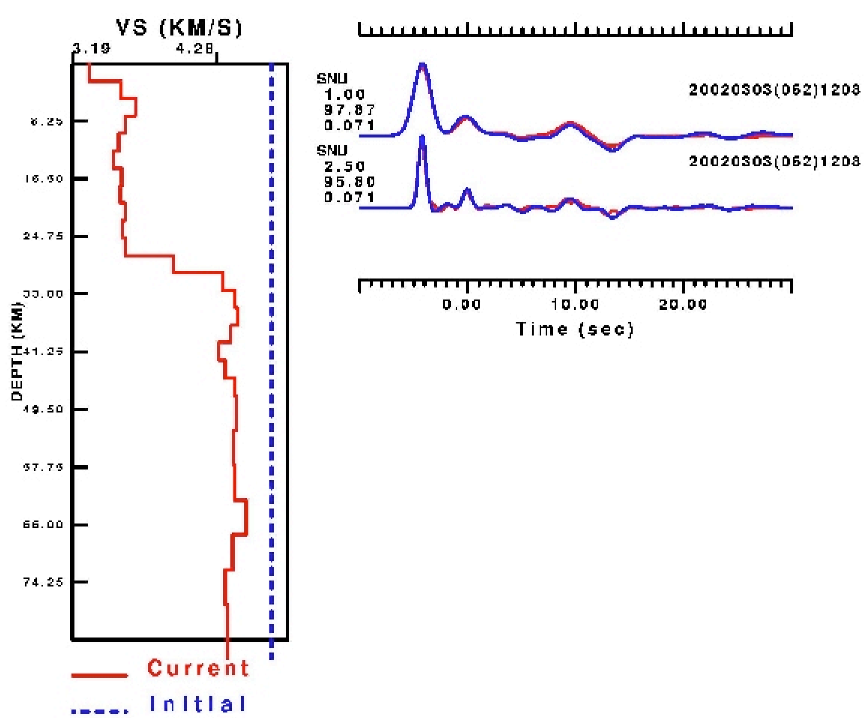

Figure 6. Inversion results using program joint96 with the same stacked receiver functions. The dispersion data are shown in Figure 7. The halfspace constraint used is weaker than above in Figure 6.

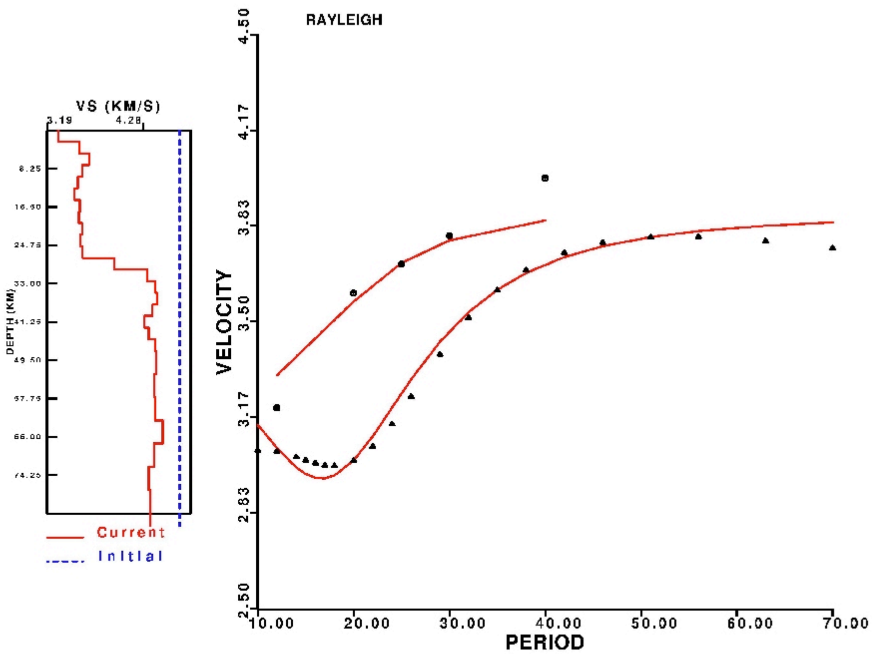

Figure 7. Rayleigh-wave groupd velocity dispersion data (Steven, 1999) and fit used with joint96. The phase velocity data are from a p-tau stack of selected broadband recordings of teleseismic surface waves.

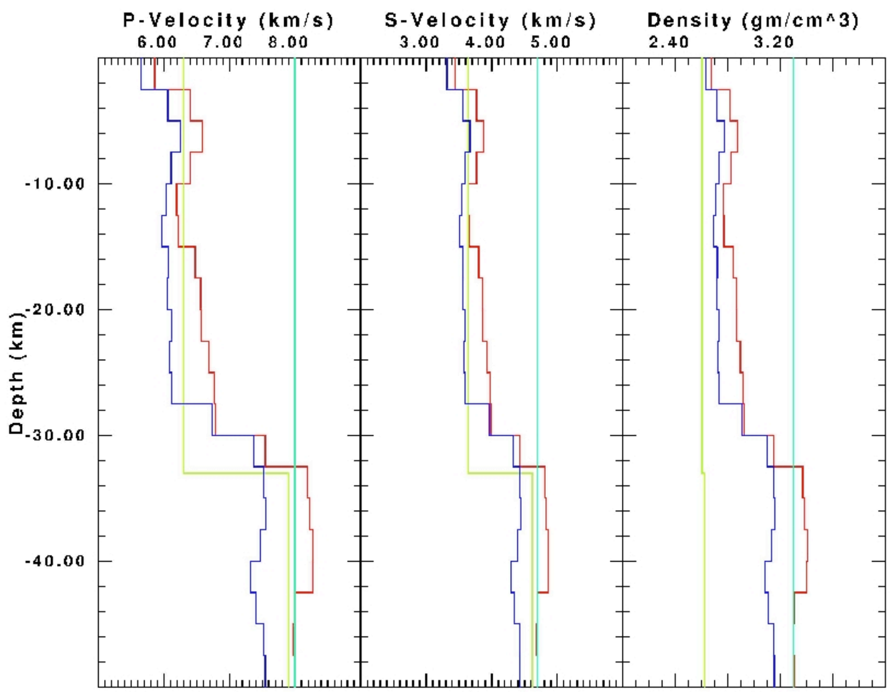

Figure 8. Overlay of models. The initial halfspace (aqua), VELEST of Song and Lee, 2001, model (yellow), the receiver function only (red) and joint inversion (blue) models are shown. The rftn96 and joint96 inversions share the Moho discontinuity at 30 km but differ in an absolute sense because of the effect of the dispersion data.

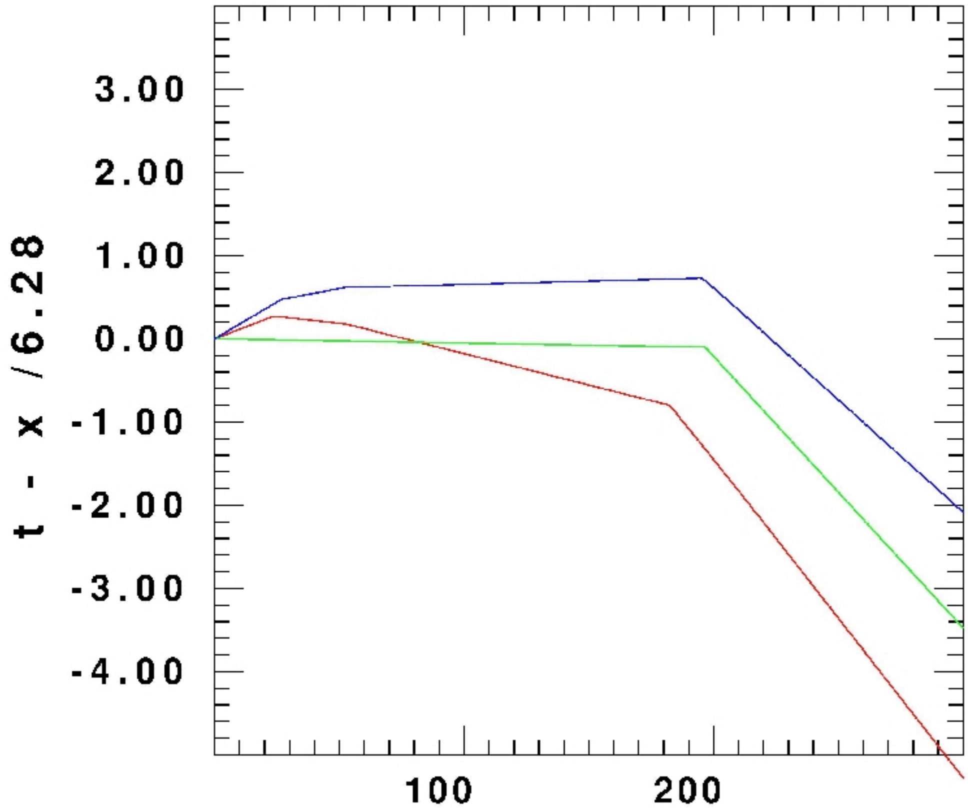

Figure 9. Comparison of predicted P-wave first arrival times for surface-focus and surface-receivers for the Song and Lee, 2001 VELEST (green), rftn96 receiver function only (red) and joint96 joint inversion models. The addition of surface wave dispersion applies a strong constraint on the receiver function inversion.